2010

Crosslinking neat ultrathin films and nanofibres of pH-responsive poly(acrylic acid) by UV radiation

Adrian Gestos
University of Wollongong, gestos@uow.edu.au

Philip G. Whitten
University of Wollongong, whitten@uow.edu.au

Geoffrey Maxwell Spinks
University of Wollongong, gspinks@uow.edu.au

Gordon G. Wallace
University of Wollongong, gwallace@uow.edu.au

Crosslinking neat ultrathin films and nanofibres of pH-responsive poly(acrylic acid) by UV radiation

Abstract

Electrospun polyelectrolyte hydrogel nanofibres are being developed for many applications including artificial muscles, scaffolds for tissue engineering, wound dressings and controlled drug release. For electrospun polyelectrolytes, a post-spinning crosslinking process is necessary for producing a hydrogel. Typically, radiation or thermal crosslinking routines are employed that require multifunctional crosslinking molecules and crosslink reaction initiators (free radical producers). Here, ultraviolet subtype-C (UVC) radiation was employed to crosslink neat poly(acrylic acid) (PAA) nanofibres and films to different crosslink densities. Specific crosslink initiators or crosslinking molecules are not necessary in this fast and simple process providing an advantage for biological applications. Scanning probe microscopy was used for the first time to measure the dry and wet dimensions of hydrogel nanofibres. The diameters of the swollen fibres decrease monotonically with increasing UVC radiation time. The fibres could be reversibly swollen/contracted by treatment with solutions of varying pH, demonstrating their potential as artificial muscles. The surprising success of UVC radiation exposure to achieve chemical crosslinks without a specific initiator molecule exploits the ultrathin dimensions of the PAA samples and will not work with relatively thick samples.

Keywords

ultrathin, neat, crosslinking, acid, acrylic, poly, responsive, ph, radiation, nanofibres, uv, films

Disciplines

Life Sciences | Physical Sciences and Mathematics | Social and Behavioral Sciences

Publication Details

Gestos, A., Whitten, P. G. & Spinks, G.M. & Wallace, G. G. (2010). Crosslinking neat ultrathin films and nanofibres of pH-responsive poly(acrylic acid) by UV radiation. Soft Matter, 6 (5), 1045-1052.

Crosslinking neat ultrathin films and nanofibres of pH-responsive poly(acrylic acid) by UV radiation

Adrian Gestos, Philip G. Whitten, Geoffrey M. Spinks* and Gordon G. Wallace

Received 13th November 2009, Accepted 23rd December 2009
First published as an Advance Article on the web 15th January 2010
DOI: 10.1039/b923831j

Electrospun polyelectrolyte hydrogel nanofibres are being developed for many applications including artificial muscles, scaffolds for tissue engineering, wound dressings and controlled drug release. For electrospun polyelectrolytes, a post-spinning crosslinking process is necessary for producing a hydrogel. Typically, radiation or thermal crosslinking routines are employed that require multifunctional crosslinking molecules and crosslink reaction initiators (free radical producers). Here, ultraviolet subtype-C (UVC) radiation was employed to crosslink neat poly(acrylic acid) (PAA) nanofibres and films to different crosslink densities. Specific crosslink initiators or crosslinking molecules are not necessary in this fast and simple process providing an advantage for biological applications. Scanning probe microscopy was used for the first time to measure the dry and wet dimensions of hydrogel nanofibres. The diameters of the swollen fibres decrease monotonically with increasing UVC radiation time. The fibres could be reversibly swollen/contracted by treatment with solutions of varying pH, demonstrating their potential as artificial muscles. The surprising success of UVC radiation exposure to achieve chemical crosslinks without a specific initiator molecule exploits the ultrathin dimensions of the PAA samples and will not work with relatively thick samples.

1 Introduction

Ultrathin crosslinked polyelectrolytes that swell in an aqueous solution, forming a hydrogel, are being developed for many applications. Biomedical examples are most common as reviewed recently,[1–3] and include particles and capsules for drug delivery and synthetic cells, fibres, assemblies of fibres and films for tissue scaffolds, wound dressings and artificial muscles. In many of these applications, a high surface area to volume ratio is desired to allow rapid response (actuators and controlled release) or maximum interaction with surrounding tissue (scaffolds and biosensors). Electrospinning is one of the simplest and most common techniques for forming high surface area membranes and recent reviews highlight the types of structures and polymers that can be formed by this method.[4–6] The membranes formed by electrospinning consist of non-woven mats of nanofibres. As the diffusion distance of molecular species through hydrogel nanofibres is much smaller than that of macroscopic hydrogels, they are ideal platforms for rapid response systems.

Hydrogels are crosslinked polymer networks typically containing more than 90% water. The crosslinks may be physical or chemical. They act to prevent the dissolution of the otherwise water-soluble polymer. The crosslinks also prevent flow of the solvated polymers, giving them the properties of a solid. Chemically crosslinked gels are normally stronger and stiffer than physically crosslinked gels as the crosslinks in the former are fixed. Control of the crosslink density is necessary for many applications as it determines the hydrogel's swollen volume as well as the key mechanical property of elastic modulus.[7] To date it has been difficult to chemically crosslink polyelectrolyte nanofibres and to control the crosslink density. Another potential problem for *in vivo* biological applications is the possible leaching of unreacted crosslinking molecules or chemical initiators, as some of these are toxic. Herein, we describe a simple method for controlling the crosslink density of ultrathin poly(acrylic acid) (PAA), a biocompatible polyelectrolyte, without the use of additional crosslinkers.

Chemical crosslinks must be formed post-fibre formation as electrospinning requires the fibre precursor to be in a liquid phase. For wet-spun hydrogel microfibres, solution based crosslinking post-treatments have been used. For example, chitosan fibres with diameters larger than 10 μm are readily crosslinked by soaking them in a solution containing glutaric aldehyde.[8] However, the same procedure fails to crosslink fibres of the same material with diameters less than 100 nm. In contrast to microfibres, the dissolution of nanofibres when immersed in a crosslinking solution is so fast that they completely dissolve prior to the development of the minimum number of crosslinks required to form a gel. Consequently, non-solution based processes are necessary to form gel nanofibres.

Thermal and radiation initiated chemical crosslinking are two process types that allow solution free crosslink formation in nanofibres. Chen and Hsieh were the first to report crosslinking of nanofibres by thermal annealing.[9] They obtained stable hydrogel fibres by spinning solutions containing PAA and polyvinyl alcohol (PVA), then annealing the fibres at 140 °C to produce ester linkages between the functional groups on the respective polymers.[9] A similar approach employing esterification at elevated temperatures has been applied by several groups

ARC Centre of Excellence for Electromaterials Science, Intelligent Polymer Research Institute, AIIM Facility, Innovation Campus University of Wollongong, NSW 2522, Australia. E-mail: geoff_spinks@uow.edu.au; Fax: +61 2 42213114; Tel: +61 2 42213010

to produce hydrogel nanofibres.[10–13] However, fibres with crosslinks formed by ester linkages between different polymers are expected to degrade upon long term immersion in water as the ester linkage is not stable. Furthermore, this approach does not allow for a wide range of crosslink densities.

UV radiation is used widely to crosslink or chemically modify a wide range of polymer systems. For most polymers a photo-initiator is necessary to generate free radicals when UV radiation is used for crosslinking. Kim *et al.* were able to employ UV radiation to form poly(2-hydroxyethyl methacrylate) (pHEMA) gel nanofibres by photo-polymerisation of oligomers in the presence of a photo-initiator during the spinning process.[14] The use of a photo-initiator is not desirable for biological applications like wound dressings where neat polymers are preferred.[15]

Some polymers contain appropriate functional groups which form radicals upon adsorption of UV radiation without a separate photo-initiator molecule being present. While potentially useful for crosslinking, this method has not been practiced. For this approach the UV penetration depth is smaller than usual due to the high density of UV absorbing functional groups preventing application to thick samples. In contrast, ultrathin polymer films, particles and fibres that contain suitable functional groups should be readily crosslinked by UV exposure. Using UV radiation to crosslink neat ultrathin polymers exploits their small thickness. Hence, a process window exists where appropriate ultrathin polymer films may be crosslinked by UV radiation but crosslinking of relatively thick films of the same polymer would be unsuccessful.

The aim of this study was to produce neat ultrathin polyelectrolyte gels with controllable swelling. We report for the first time the use of short wave ultraviolet subtype-C (UVC) radiation to produce hydrogel nanofibres without the use of photo-initiator or other crosslinking agents. We demonstrate the process to crosslink neat PAA nanofibres and ultrathin films. Scanning probe microscopy (SPM) was used to characterise the shape, size and elasticity of the crosslinked nanofibres immersed in an electrolyte over a range of pH and crosslink densities. The same crosslinking method could be universally applied to any ultrathin polymer layer that contains appropriate functional groups for the UVC induced crosslinking.

2 Methods

2.1 Materials

PAA ($M_w \approx 450\,000$ g/mol) was purchased from Polysciences, Inc. Poly(allylamine hydrochloride) (PAH, $M_w \approx 70\,000$ g/mol) and citric acid were purchased from Sigma-Aldrich. Disodium hydrogen phosphate heptahydrate was purchased from Fluka. Concentrated sulfuric acid, concentrated hydrochloric acid and 35% hydrogen peroxide were purchased from AJAX Finechem. 3-Aminopropyltriethoxysilane (APTES) was purchased from Gelest. Buffers of pH 3 and pH 8 were prepared by mixing different ratios of 0.1 M citric acid and 0.2 M disodium hydrogen phosphate heptahydrate. All chemicals were used as received. Aqueous solutions were prepared using Milli-Q water (resistivity of 18.2 MΩ cm).

2.2 Amine functionalisation of glass slides

Glass slides were used as a substrate to support the nanofibres. The slides were cleaned and hydroxylated by immersion in freshly made piranha solution ($3H_2SO_4 : 1H_2O_2$ by volume) for 1 h then rinsed with copious amounts of Milli-Q followed by acetone then blown dry with nitrogen (care must be taken not to mix acetone and piranha solution). The cleaned slides were then placed into a 3% v/v solution of APTES in acetone for 20 min with slow stirring. The glass slides were then removed from the solution and rinsed with copious amounts of acetone, blown dry with N_2(g) and cured in an oven at 110 °C for 10 min.

2.3 Fabrication of electrospun and crosslinked fibres

Fibres were electrospun from a solution of 8% w/v PAA. A syringe pump (KD Scientific) was used to provide a flow rate of 0.5 ml h^{-1}. A potential of 10 kV was applied by connecting the power supply (Gamma High Voltage Research) to the syringe tip. An additional plastic tube (purchased from Polymicro Technologies) was inserted into the syringe to reduce the internal diameter to 140 μm. The working distance between the syringe tip and aluminium foil grounded collector was 180 mm. An amine functionalised glass slide was placed on top of the aluminium foil for easy collection of fibres ready for crosslinking and analysis. The electrospun fibre coated glass slides were then exposed to UVC radiation (UVO cleaner, Jelight Company Inc. Model No. 42-220) for pre-determined times at a distance of 40 mm from the mercury lamp. The low pressure mercury vapour lamp used for the UVC radiation emits a light intensity of 24.3 mW cm^{-2} at a wavelength of 254 nm at 40 mm from the lamp. The light intensity was measured using a thermopile detector (Newport 818P-010-12). Where stated, a nitrogen atmosphere was used for the UVC radiation.

2.4 PAA nanofibre and thin film characterisation

Thin films and fibres were characterised by optical microscopy, SPM, UV-Visible spectroscopy and FTIR. A JPK Nanowizard II atomic force microscope mounted on a Nikon TE 300/2000 inverted optical microscope and Halcyonics micro 40 vibration isolation unit was used for SPM characterisation. Gold coated silicon nitride triangular cantilevers (Veeco Instruments) were used. All of the SPM imaging was conducted in contact mode. The UV-Visible spectroscopy was carried out with a Shimadzu UV-1601 on a film of PAA drop-cast onto quartz that was then dried under vacuum. FTIR was carried out using a Shimadzu IRPrestige-21 with PAA drop-cast onto a CaF_2 tablet.

Each nanofibre sample was imaged over a 400 μm^2 scan area. The same regions of fibres were imaged when dry and then consecutively over six electrolyte changes cycling between pH 3 and pH 8. The volume change due to swelling was obtained from two line traces taken on each image (Fig. 1). Each line trace was defined at, or a specific distance from, a crossover point of two fibres to ensure that the same location was measured each time. The volume swelling ratio (S_v) was calculated in each environment against the dry volume by measuring the cross-section area of each fibre and assuming that the length is constant. The height and width of the fibres were also taken over a minimum of 10 points for each image and used as a measure of fibre

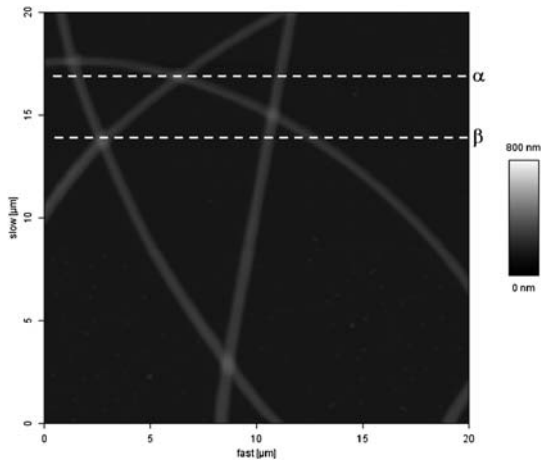

Fig. 1 Typical SPM image of dry PAA nanofibres. Traces taken at the dashed lines labelled 'α' and 'β' were used to calculate the volume change of the fibres over consecutive images.

degradation. The SPM tip widths were ignored when measuring the width of the fibres as they are at least an order of magnitude less than the fibre widths.

Force–indentation curves were performed for a qualitative measure of the hydrogel stiffness.

To image the samples in pH buffer, a 1 mm thick silicone chamber gasket (Coverwell) with a 20 mm diameter internal well was applied over the section of fibres of interest on the glass slide. The SPM imaging tip was then lowered into the liquid with the meniscus surrounding the cantilever holder so that both the cantilever and sample were immersed in electrolyte when the images were recorded.

2.5 Micropatterning of PAA thin films

A thin film of PAA was formed by spin casting a solution of 2% w/v PAA in water onto a silicon wafer at 1500 rpm. TEM grids (copper, 300 mesh purchased from ProSciTech) were used as a mask by placing on top of the film which was then exposed to UVC radiation in the presence of oxygen for 5 min. The TEM grids were then removed and the sample soaked in Milli-Q water for 24 h that had been adjusted to pH 2 with a few drops of concentrated HCl as a precaution to prevent the crosslinked portion of the PAA film swelling excessively and possibly dislodging from the silicon wafer. The sample was then dried and imaged by optical microscopy and SPM.

2.6 Fixing of multilayer films

Quartz slides were functionalised with APTES using the same method for glass slides in Section 2.2. A functionalised quartz slide was then placed into an aqueous solution of 1 mg ml^{-1} PAA for 5 min, rinsed thoroughly with Milli-Q water and placed into an aqueous solution of 0.5 mg ml^{-1} PAH for 5 min. The pH of the solutions was not adjusted as both PAA and PAH are partially charged when added to Milli-Q water. After deposition of each bilayer the film was dried under a nitrogen stream and a UV-Vis spectrum was obtained. After 6 bilayers were deposited on the quartz slide it was immersed into a 0.1 M NaOH solution for 10 min then rinsed with milli-Q water and dried under a nitrogen stream. This deprotonates the PAH leaving it with no charge and destabilises the multilayer film. An additional quartz slide with 6 bilayers was treated with UVC radiation for 8 min (4 min for each side of the slide) followed by soaking in 0.1 M NaOH for 10 min then rinsing and drying. The crosslinking of neat PAH was tested by spin coating a silicon wafer with an 8% w/v solution at 3000 rpm for 50 s, exposing to UVC radiation in air for 15 min then testing for solubility by soaking in NaOH for 10 min.

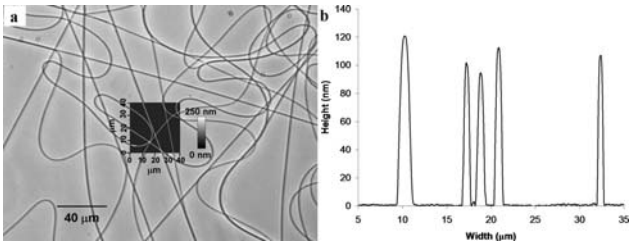

Fig. 2 (a) Optical image of dry electrospun PAA fibres with SPM image overlaid in the centre and (b) representative single scan taken from the SPM image showing cross-sections of 5 fibres.

3 Results and discussion

Electrospun PAA fibres were deposited at low density on the glass slides, allowing easy identification of the fibres by an inverted optical microscope (Fig. 2a). The dry electrospun PAA fibres had an ellipsoidal cross-sectional shape with an average height and width of 125 nm and 750 nm respectively, as determined from the SPM trace (overlay in Fig. 2a and b). These are consistent with those reported by Li and Hsieh for electrospun PAA.[16]

3.1 Effects of UVC radiation on the morphology and chemical structure of PAA electrospun fibres

There was a significant decrease in the observed fibre's cross-sectional area by increasing UVC radiation time from 5 to 25 min (Fig. 3). No significant change in the dry fibre's cross-sectional area was observed for UVC exposure times less than 5 min. The observed reduction in cross-sectional area for radiation exposure

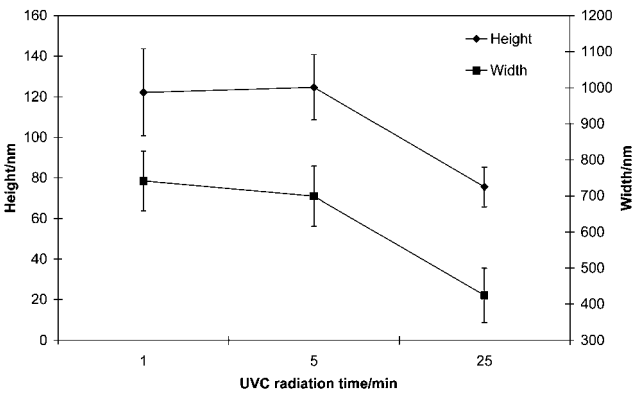

Fig. 3 Dry fibre height and width averaged over points taken from triplicate samples at 1, 5 and 25 min UVC radiation time in an air atmosphere with error bars indicating one standard deviation. These fibres were imaged dry after UVC irradiation.

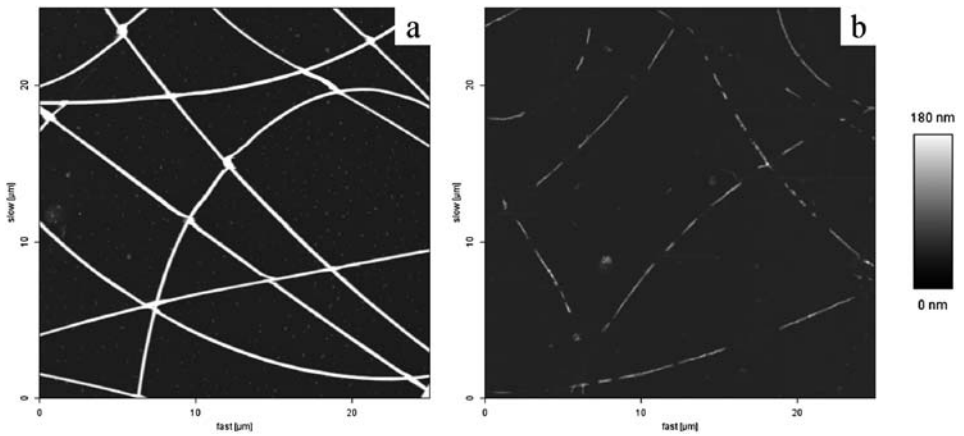

Fig. 4 SPM height image of PAA fibres UVC treated for 25 min in a (a) nitrogen atmosphere and (b) in an air atmosphere.

times greater than 5 min is due to loss of volatile decomposition products to the atmosphere. The exposure of PAA nanofibres to UVC radiation in the presence of air resulted in a gradual decomposition of PAA.

In contrast to an air atmosphere, exposure of PAA nanofibres to UVC radiation in a nitrogen atmosphere resulted in no observable change in fibre cross-sectional area for radiation exposure times of up to 25 min. This contrast in atmosphere dependent stability of PAA is evident by SPM imaging of the fibres post-UVC exposure (Fig. 4). Severe degradation of the air-exposed samples is clearly evident (Fig. 4b).

It is expected that PAA, like most polymers, should degrade when exposed to UVC radiation in an oxygen containing atmosphere.[17–19] It was also expected that the volume loss associated with this degradation would not be apparent until after an initial period of UVC exposure. For the system presented here, UVC exposure longer than 5 min is necessary to produce molecular fragments through chain scission and oxidation reactions that are small enough to be volatile and evolve from the solid fibre. These results are consistent with diffusion limited oxidation, where the rate of oxygen consumption in the PAA is much greater than the rate at which oxygen can be resupplied by diffusion from the surrounding air atmosphere.[20] Hence, equilibrium oxidation is expected at the nanofibre's surface but reduced or non-existent oxidation occurs in the fibre interior.[20] In a nitrogen atmosphere, the PAA fibres do not degrade, as oxidation will not occur without oxygen being present.

3.1.1 Gelation mechanism. UVC radiation of the PAA nanofibres in either air or nitrogen atmospheres for the exposure times studied (1–25 min) resulted in insoluble fibres that adhered to the amine functionalised glass substrate and swelled when placed in pH 8 buffer. The fact that the fibres remained attached to the substrate indicates that the fibres were crosslinked to some degree through their entire thickness by the UVC treatment. Uncrosslinked material would dissolve and cause the fibres to detach. The UVC exposed fibres did not dissolve even when immersed in water for one week. In contrast, PAA fibres not exposed to UVC radiation dissolved rapidly when immersed in water. Hence, the PAA nanofibres were successfully crosslinked by the UVC radiation.

The use of UVC radiation to crosslink bulk polymer samples without the aid of an initiator has not previously been reported. In a similar approach, Wu *et al.* recently added azido bearing functional groups to PAA, which forms a free radical when exposed to UVA radiation with a wavelength of 365 nm.[21] The free radicals formed then reacted with neighbouring molecules in multilayered films. The key disadvantage of Wu *et al.*'s approach, compared to the one presented here, is that there are additional steps required to attach the azido bearing groups to the PAA. A significant advantage of Wu *et al.*'s approach is that the crosslink density is determined by the density of azido groups and becomes independent of radiation time once saturation has been reached.

UV radiation exhibits a small penetration depth due to its low energy. As such, UVC radiation is normally considered as a surface effect and would produce a crosslinked skin on a thick polymer sample.[22] In the situation presented here, the concentration of the UVC absorbing group is high, so it is expected that the crosslinking is localised over a length scale in the order of 10–100 μm.[23] A gradient in crosslink density may occur through the thickness of the nanofibres due to a decrease in light intensity with penetration depth. However, quantification of the crosslink density at small length scales is difficult and the variation in crosslinking of PAA using UVC radiation is unknown at this time. This area is the subject of ongoing research. The results clearly demonstrate that when the thickness of the sample approaches the nanoscale, then it is seen that UVC radiation can be exploited as a through-thickness crosslinking technique. Consequently, nano-thick polymers may be crosslinked by UVC radiation analogous to samples many orders of magnitude thicker being crosslinked by high energy radiation like γ-radiation,[15] or electron beams. As such, UVC radiation may find commercial application for crosslinking membranes formed by electrospinning that are used for biomedical applications. UVC radiation may also be applied to crosslink ultrathin polymer films, particles or capsules.

The exact reaction path for crosslinking the PAA is difficult to isolate. We believe the crosslinks to be chemical bonds and not physical bonds as they are stable at all solution pH's studied, and the swollen fibres are highly elastic. In a previous degradation study the crosslinking of PAA by UVC was noted.[24] It is known

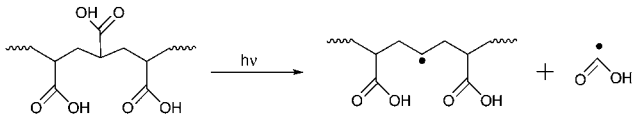

Scheme 1 UVC induced Norrish I α-cleavage of the carboxylic acid group from PAA.

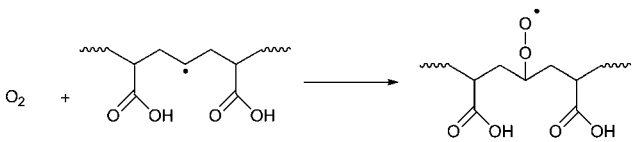

Scheme 2 Radical scavenging by oxygen.

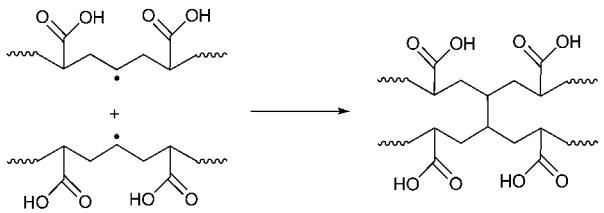

Scheme 3 Possible scheme for the UVC induced crosslinking of PAA in the absence of oxygen.

that irradiation of PAA by 248 nm wavelength UVC primarily leads to Norrish I α-cleavage of the carboxylic acid group (Scheme 1) which can then either recombine, degrade the polymer through β-scission or form inter- and intra-molecular crosslinks.[25]

It is clear that competing processes leading to both chain scission and crosslinking are taking place when the PAA fibres are exposed to UVC in air. At the surface region oxygen reacts with the radicals on the PAA (Scheme 2) which undergoes further reactions leading to chain scission and finally, the production of low molecular weight volatile components.[26] In the interior there is minimal oxygen and chemical crosslinking is the dominant process (Scheme 3). In contrast, in the nitrogen atmosphere chemical crosslinking at both the surface and the interior is the dominant process. It should be noted that chemical crosslinking is more dominant here than for polymer solutions as the polymer chains are in close proximity to each other.[27]

Further evidence for the chemical transformation of the PAA upon UVC radiation is the change in the FTIR spectrum of a drop-cast PAA film with different UVC exposure times (Fig. 5). The broad peak from 3700 cm^{-1} to 2400 cm^{-1} is due to the O–H stretch of a carboxylic acid while the sharp peak within that region from 3000 cm^{-1} to 2850 cm^{-1} is due to the C–H stretch of an alkane.[28] By integrating the area under each region and calculating the ratio of the two, a quantifiable measure of the change in chemical composition was obtained. The inset in Fig. 5 shows an inverse relationship between the amount of O–H groups relative to the C–H groups for UVC exposure times up to 40 min (58.3 J cm^{-2}). This relationship supports the proposed reaction scheme where carboxylic acid groups are lost and carbon–carbon bonds are formed.

For practical applications, a high ratio of crosslinking to chain scission is desirable. As oxygen is a reagent for chain scission reactions for many polymers, excluding it from the polymer undergoing irradiation is essential to efficient crosslinking. In the absence of oxygen, experimental variables including radiation wavelength, polymer thickness, radiation intensity and irradiation time will determine if and where crosslinks form, but they are unlikely to alter the ratio of crosslinking to chain scission for PAA.

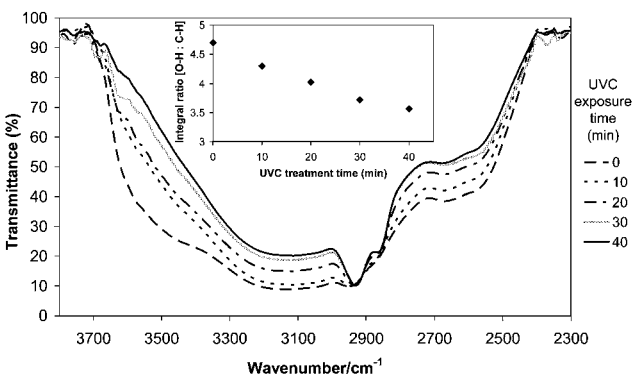

Fig. 5 FTIR spectra of PAA with increasing UVC exposure time and inset showing the ratio of the integral intensity of the carboxylic acid O–H stretch (3700–2400 cm^{-1}) to the alkane C–H stretch (3000–2850 cm^{-1}).

3.2 Effects of UVC radiation on the pH-responsive swelling of PAA electrospun fibres

The swollen cross-section of PAA electrospun fibres exposed to UVC radiation in air for 5 and 25 min at pH 3 and pH 8 was successfully measured by SPM. In contrast, the PAA fibres exposed to UVC radiation for 1 min were too soft to be reliably imaged by SPM with the cantilevers that were available. The difference in sample stiffness and hence, imaging quality, is most likely due to the difference in crosslink densities, with the softer sample having a lower crosslink density. The 1 min exposed sample was of similar or lower stiffness than the SPM cantilever being used, thereby leading to difficulties in imaging. This observation indicates that the increasing UVC time from 1 to 5 min increases the stiffness and hence the crosslink density of the PAA fibres.

The crosslinked PAA nanofibres exhibited substantial changes in volume when the immersion solution was changed from pH 8 to pH 3. The fibres swelled in mildly alkaline solution (pH 8) and shrunk in acidic solution (pH 3). The dimensional changes were reproducible, as shown in Fig. 6, which shows individual scans taken over the same region on 3 fibres in the dry state and following 3 consecutive pH switching cycles. The dashed lines in Fig. 1 show the sections analysed.

The UVC treatment time greatly affected the extent of change in swelling induced by pH switching. The 5 min UVC treated PAA nanofibres swelled to ~1.6 times the dry volume in pH 3 and ~7.6 times (87% electrolyte by volume) the dry volume in pH 8 (Fig. 7). Swelling ratios decreased with increasing UVC treatment time from 5 to 25 min (that is 7.3 to 36.5 J cm^{-2}) (Fig. 7). In pH 3, the 25 min UVC treated fibre attained swelling of S_v ~0.91; in pH 8 these values were slightly higher at S_v ~2.0.

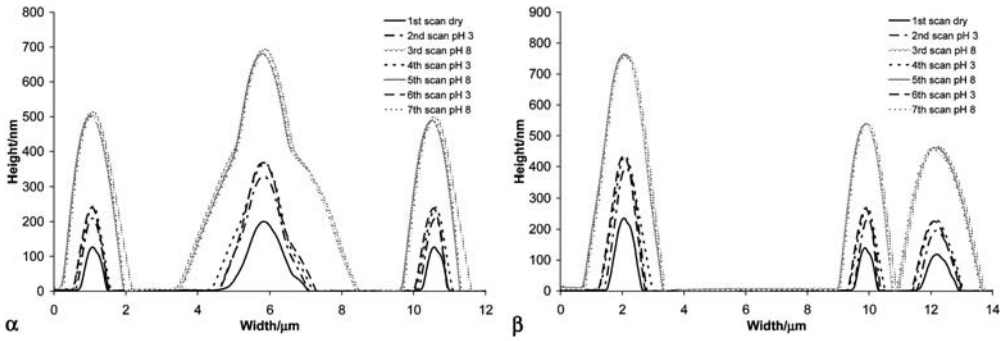

Fig. 6 Representative traces taken from consecutive SPM images in different environments. These traces were taken from the positions shown by the dashed lines (α and β) in Fig. 1 for PAA nanofibres exposed to UVC radiation for 5 min in air.

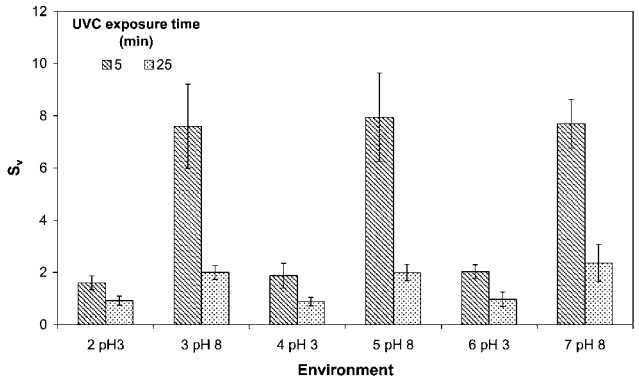

Fig. 7 S_v over traces taken from three samples at both 5 and 25 min UVC treatment time and after successive changes in solution pH. Error bars indicate one standard deviation in swelling ratio.

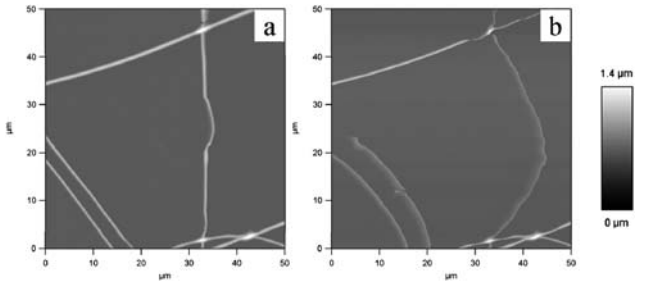

Fig. 8 SPM height image of PAA nanofibres irradiated by UVC for 5 min and then immersed in a pH 3 electrolyte on (a) the first scan showing a mostly stationary fibre from top to bottom and (b) the fourth scan showing the same fibre being snagged and dragged whilst anchored at the two crossover points.

The observed reduction in swelling ratio for increasing UVC radiation dose is likely due to an increase in crosslink density. An increase in crosslink density introduces more constrained junctions into the network and a reduction in swelling.[29,30] Somewhat unexpectedly, the 25 min treated PAA sample showed an initial shrinkage when first immersed in solution (pH 3). It is likely that leaching of low molecular weight soluble fragments and uncrosslinked PAA may counteract the swelling and produce a small reduction in dimensions. Subsequent pH switching produced the expected swelling and shrinkage in a reproducible manner.

3.3 Effects of UVC radiation on the mechanical properties of PAA electrospun fibres

The fibres exposed to UVC radiation for 5 min showed outstanding robustness as evidenced by the occasional "snagging and dragging" of fibres by the SPM tip during imaging (Fig. 8). Sections of the fibres, anchored at their crossover junctions could be dragged considerable distances without failure. In fact, within the limits of the range of motion offered by our SPM, we were unable to break a fibre while stretching it between the junction points to tensile strains greater than 120%. While we are now conducting controlled experiments to quantify the toughness and modulus of the nanofibres, these preliminary experiments demonstrate that the UVC crosslinked PAA nanofibres exhibit substantial mechanical resilience in the wet state, which is highly unusual for hydrogels.

Indentation tests of the SPM tip into the individual fibres also indicate that the crosslink density of the fibres is much larger for 25 min than it is for 5 min exposure to UVC radiation. The 5 min PAA fibres at pH 3 give an indentation stiffness of ~0.10 N m^{-1}, much lower than that of the 25 min sample at >0.19 N m^{-1} (Fig. 9). As the cantilever stiffness (~0.2 N m^{-1}) is similar to that measured for the 25 min sample, only the minimum stiffness can be inferred. Thus, in qualitative terms, PAA exposed to UVC radiation for 25 min is at least twice as stiff as the same material

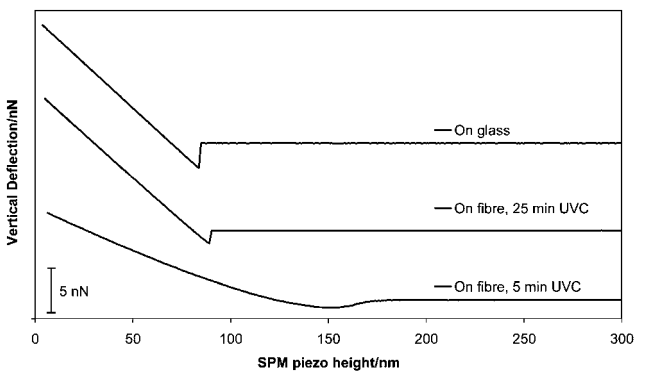

Fig. 9 SPM approach indentation curves carried out in a pH 3 environment on different surfaces.

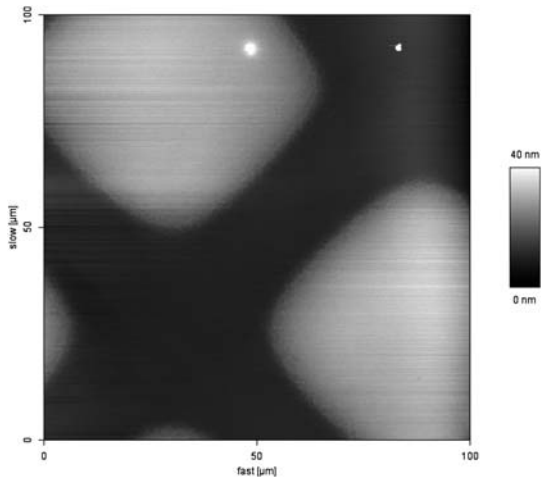

Fig. 10 SPM height image of a dry, thin PAA film, UVC treated while masked with a TEM grid then soaked in acidic solution to remove uncrosslinked PAA, revealing the pattern of the mask.

exposed to UVC radiation for just 5 min. This change in stiffness is consistent with an increase in crosslink density.[7]

3.4 Further applications

The inherent simplicity of this method for crosslinking thin films or fibres of PAA lends itself to a variety of applications or extensions of the method. Two examples are described below.

3.4.1 Micropatterning of PAA thin films. The crosslinking mechanism proposed should be localised to regions exposed to UVC radiation. Consequently, a mask or focused laser UVC radiation can be used to pattern complex shapes into PAA films. To demonstrate this effect, we employed TEM grids as masks on top of a PAA spin coated film.

The SPM height image taken in the masked area shows a clear pattern in the PAA thin film that matches the TEM grid used as a mask (Fig. 10). The raised areas represent the gaps in the grid where the PAA film was exposed to UVC radiation and crosslinked. The valleys correspond to the wires of the TEM grid where the film was not crosslinked and dissolved away after being soaked in the acidic solution. The application of a mask proves that the crosslinking reaction is confined to regions exposed to UVC radiation.

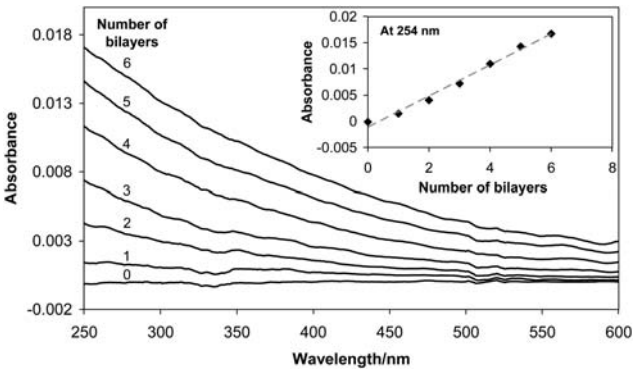

Fig. 11 UV-Vis spectra of the PAA–PAH multilayer film increasing in absorbance with number of bilayers.

3.4.2 Stabilisation of multilayer films. Multilayer films formed by the layer-by-layer technique are an ideal thickness to be crosslinked by UVC radiation, where one of the layers is PAA or another polyelectrolyte with appropriate functional groups. Multilayer films are currently being developed for many applications including drug delivery systems and functional coatings. Layer-by-layer systems are typically two component systems, where at least one of the two components is a weakly charged polyelectrolyte.

To demonstrate the stabilisation of multilayer films, PAA and PAH were employed for the alternate layers. PAH is a polyelectrolyte with a positive charge when dissolved in milli-Q water that also crosslinks when exposed to UVC radiation. The crosslinking of PAH ultrathin films was evident from their insolubility in 0.1 M NaOH after exposure to UVC radiation.

The evolution of the multilayer film, formed by alternatively dip coating in PAA and PAH, can clearly be seen in the UV-Vis spectrum taken after the deposition of each bilayer (Fig. 11). The inset in Fig. 11 shows that the increase in absorbance with number of bilayers is linear, suggesting that the same amount of material is being deposited each time. Soaking an untreated multilayer film in 0.1 M NaOH for 10 min completely removes the film from the quartz slide (Fig. 12a). However, after UVC treatment for 8 min, the film has been fixed and is not removed after immersion in 0.1 M NaOH (Fig. 12b). It is likely that crosslinks have formed within and between the PAA and PAH layers. The crosslinking mechanism contrasts that proposed by Wu *et al.* for PAA modified with photoreactive azido groups.[21]

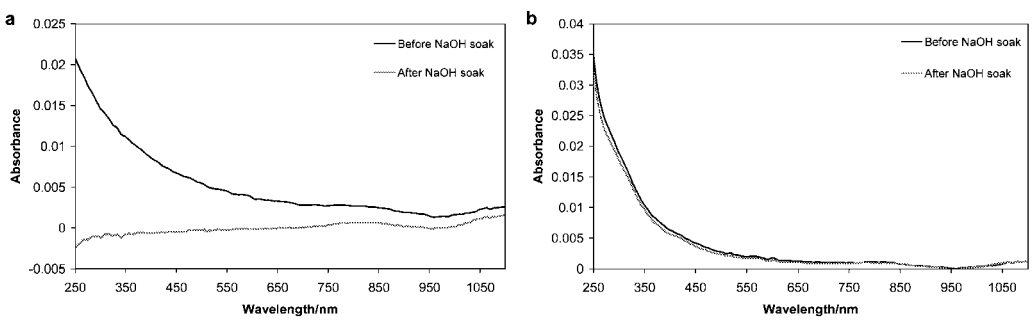

Fig. 12 UV-Vis spectrum of a 6 bilayer PAA–PAH film on quartz before and after soaking in 0.1 M NaOH for 10 min (a) with no UVC exposure and (b) after 8 min of UVC exposure.

Here we have achieved a similar result without needing to modify the PAA but simply employing a higher energy (smaller wavelength) UV radiation that forms free radicals in both polyelectrolytes.

4 Conclusions

Neat PAA hydrogel nanofibres were produced by the simple process route of electrospinning followed by exposure to UVC radiation. The UVC radiation forms chemical crosslinks through free radical reactions. In the absence of oxygen, the nanofibres remain undegraded to treatment times of 25 min (36.5 J cm^{-2}). The crosslink density, and hence the swelling and mechanical properties of the fibres, is readily controlled by employing different UVC radiation doses. The crosslinked fibres were pH-responsive, swelling and contracting repeatedly in response to a pH change. The fibres were also mechanically robust, being able to be stretched to at least 120% strain without failure. Localised crosslinking could be achieved using masks or other optical methods. The method was also used to crosslink PAH and multilayer thin films where one or more of the layers contained a UV sensitive polymer.

The approach presented herein can be readily applied to produce hydrogel nanofibre membranes for applications including artificial muscles and tissue engineering scaffolds. Indeed, UVC radiation sensitive polymers may be crosslinked to form films, fibres, membranes, particles or capsules without the aid of photoinitiators. This approach is ideal for medical applications due to its inherent purity and simplicity.

Acknowledgements

The authors acknowledge the Australian Research Council for financial support through its Centres of Excellence program. The authors also are grateful to Dr Philip Barker for useful discussions.

References

1 D. Liang, B. S. Hsiao and B. Chu, *Adv. Drug Delivery Rev.*, 2007, **59**, 1392–1412.
2 J. Venugopal and S. Ramakrishna, *Appl. Biochem. Biotechnol.*, 2005, **125**, 147–157.
3 G. H. Kim and H. Yoon, *Appl. Phys. A: Mater. Sci. Process.*, 2008, **90**, 389–394.
4 Y. Filatov, A. Budyka and V. Kirichenko, *Electrospinning of Micro- and Nanofibers: Fundamentals in Separation and Filtration Processes*, Begell House, Redding CT USA, 2007.
5 D. Li and Y. Xia, *Adv. Mater.*, 2004, **16**, 1151–1170.
6 W. E. Teo and S. Ramakrishna, *Nanotechnology*, 2006, R89.
7 M. Rubinstein, R. H. Colby, A. V. Dobrynin and J.-F. Joanny, *Macromolecules*, 1996, **29**, 398–406.
8 G. M. Spinks, S. R. Shin, P. G. Whitten, S. I. Kim, S. J. Kim and G. G. Wallace, *Sens. Actuators, B*, 2006, **115**, 678–684.
9 H. Chen and Y.-L. Hsieh, *J. Polym. Sci., Part A: Polym. Chem.*, 2004, **42**, 6331–6339.
10 L. Li and Y.-L. Hsieh, *Polymer*, 2005, **46**, 5133–5139.
11 X. Jin and Y.-L. Hsieh, *Macromol. Chem. Phys.*, 2005, **206**, 1745–1751.
12 X. Jin and Y.-L. Hsieh, *Polymer*, 2005, **46**, 5149–5160.
13 H. Liu, M. Zhen and R. Wu, *Macromol. Chem. Phys.*, 2007, **208**, 874–880.
14 S. H. Kim, S.-H. Kim, S. Nair and E. Moore, *Macromolecules*, 2005, **38**, 3719–3723.
15 J. M. Rosiak, P. Ulanski, L. A. Pajewski, F. Yoshii and K. Makuuchi, *Radiat. Phys. Chem.*, 1995, **46**, 161–168.
16 L. Li and Y.-L. Hsieh, *Polymer*, 2005, **46**, 5133–5139.
17 H. Y. Nie, B. B. Walzak and N. S. Mcintyre, *Appl. Surf. Sci.*, 1999, **144–145**, 627–632.
18 D. O. H. Teare, C. Ton-That and R. H. Bradley, *Surf. Interface Anal.*, 2000, **29**, 276–283.
19 C. Decker, in *Handbook of polymer science and technology*, ed. N. P. Cheremisinoff and M. Dekker, New York, 1989, vol. 3, Applications and processing operations.
20 K. T. Gillen and R. L. Clough, in *Radiation effects on polymers*, ed. R. L. Clough and S. W. Shalaby, American Chemical Society, Washington, DC, 1991, ch. 28, pp. 457–472.
21 G. Wu, F. Shi, Z. Wang, Z. Liu and X. Zhang, *Langmuir*, 2009, **25**, 2949–2955.
22 H. Kaczmarek, *Polymer*, 1996, **37**, 189–194.
23 G. Terrones and A. J. Pearlstein, *Macromolecules*, 2001, **34**, 3195–3204.
24 H. Kaczmarek, A. Kaminska, M. Swiatek and J. F. Rabek, *Angew. Makromol. Chem.*, 1998, **261–262**, 109–121.
25 N. V. Lebedeva and M. D. E. Forbes, *Macromolecules*, 2008, **41**, 1334–1340.
26 D. Feldman, *J. Polym. Environ.*, 2002, **10**, 163–173.
27 S. Zhu, R. H. Pelton and A. E. Hamielec, *Eur. Polym. J.*, 1998, **34**, 487–492.
28 R. M. Silverstein, F. X. Webster and D. J. Kiemle, *Spectrometric identification of organic compounds*, John Wiley & Sons, Hoboken, NJ, 7th edn, 2005.
29 R. Skouri, F. Schosseler, J. P. Munch and S. J. Candau, *Macromolecules*, 1995, **28**, 197–210.
30 G. M. Eichenbaum, P. F. Kiser, A. V. Dobrynin, S. A. Simon and D. Needham, *Macromolecules*, 1999, **32**, 4867–4878.

